CONFERENCE PRE-PRINT

EXPERIMENTAL OBSERVATION OF ZONAL FLOW-LIKE OSCILLATION IN CHINESE FIRST QUASI-AXISYMMETRIC STELLARATOR-TEST DEVICE

X. Chen
Institute of Fusion Science, School of Physical Science and Technology, Southwest Jiaotong University, Chengdu, People's Republic of China
Email: marguerite@my.swjtu.edu.cn

J. Cheng
Institute of Fusion Science, School of Physical Science and Technology, Southwest Jiaotong University, Chengdu, People's Republic of China

Y. Xu
Institute of Fusion Science, School of Physical Science and Technology, Southwest Jiaotong University, Chengdu, People's Republic of China

H. F. Liu
Institute of Fusion Science, School of Physical Science and Technology, Southwest Jiaotong University, Chengdu, People's Republic of China

X. Q. Wang
Institute of Fusion Science, School of Physical Science and Technology, Southwest Jiaotong University, Chengdu, People's Republic of China

J. Chen
Institute of Fusion Science, School of Physical Science and Technology, Southwest Jiaotong University, Chengdu, People's Republic of China

W. M. Xuan
Institute of Fusion Science, School of Physical Science and Technology, Southwest Jiaotong University, Chengdu, People's Republic of China

J. Huang
Institute of Fusion Science, School of Physical Science and Technology, Southwest Jiaotong University, Chengdu, People's Republic of China

H. Liu
Institute of Fusion Science, School of Physical Science and Technology, Southwest Jiaotong University, Chengdu, People's Republic of China

X. Zhang
Institute of Fusion Science, School of Physical Science and Technology, Southwest Jiaotong University, Chengdu, People's Republic of China

J. F. Shen
Institute of Fusion Science, School of Physical Science and Technology, Southwest Jiaotong University, Chengdu, People's Republic of China

J. Hu
Institute of Fusion Science, School of Physical Science and Technology, Southwest Jiaotong University, Chengdu, People's Republic of China

H. Lan
Institute of Fusion Science, School of Physical Science and Technology, Southwest Jiaotong University, Chengdu, People's Republic of China

A. Shimizu

National Institute for Fusion Science, National Institutes of Natural Sciences
Toki, Japan
The Graduate University for Advanced Studies, SOKENDAI
Toki, Japan

M. Isobe
National Institute for Fusion Science, National Institutes of Natural Sciences
Toki, Japan
The Graduate University for Advanced Studies, SOKENDAI
Toki, Japan

S. Okamura
National Institute for Fusion Science, National Institutes of Natural Sciences
Toki, Japan

M. Shoji
National Institute for Fusion Science, National Institutes of Natural Sciences
Toki, Japan

K. Ogawa
National Institute for Fusion Science, National Institutes of Natural Sciences
Toki, Japan
The Graduate University for Advanced Studies, SOKENDAI
Toki, Japan

D. Yin
Anhui Link Future Technology Co., Ltd
Hefei, China

C. Tang
Institute of Fusion Science, School of Physical Science and Technology, Southwest Jiaotong University,
Chengdu, People's Republic of China

Abstract

A low frequency electrostatic oscillation has been observed for the first time in the optimized Chinese First Quasi-axisymmetric Stellarator (CFQS) plasma. This oscillation flow, peaking at a central frequency of 1.0 kHz, exhibits a finite radial scale of approximately 3-4 cm (comparable to several ion gyroradii) and displays strong long-range correlation as evidenced by measurements from two floating potentials toroidally separated by 200 cm. Bicoherence analysis further confirms that the oscillation originates from nonlinear three-wave coupling with ambient turbulence in the frequency range of f~10-150 kHz. These observed characteristics align qualitatively with the theoretically predicated low-frequency zonal flows (LFZF). Further investigation reveals an inverse correlation between the amplitude of LFZF-like structure and local particle flux, suggesting its significant role in suppressing ambient turbulence. This study provides direct experimental evidence of zonal flow presence in an optimized quasi-axisymmetric stellarator and highlights its importance in turbulence regulation. The findings offer new insights for the validation of model aimed at minimizing turbulent transport in future advanced stellarator designs.

1. INTRODUCTION

Achieving and sustaining high plasma performance is a central challenge in magnetic-confinement fusion, because cross-field turbulent transport can dominate energy and particle losses and thus set operational limits for confinement [1]. Zonal flows, characterized as axisymmetric E × B flows with large poloidal and toroidal wavelengths, play a critical role in regulating turbulence and mitigating anomalous transport [2]. In tokamaks, extensive experimental evidence has demonstrated the coexistence of low frequency zonal flow (LFZF) with geodesic acoustic mode (GAM) and their function as energy sinks for turbulence. For example, Zero-mean-frequency (ZMF) ZF were observed in DIII-D in the core region (~0.6-0.9) with a short radial coherence length ($L_{c,r}$~$1.4\ cm$), consistent with theoretical predictions [3]. In HL-2A, low-frequency ZF were reported alongside GAM, both generated via nonlinear coupling with ambient turbulence [4]. Stationary ZF have also been identified in JET, where they correlate with turbulence reduction during L-H transitions and is important for development of the pedestal [5]. Other observations from HT-7[6], JFT-2M[7], TEXTOR[8], EAST[9], Alcator C-Mod[10], and MAST[11] confirmed that ZF are ubiquitous in axisymmetric magnetic configuration, such as

tokamaks, contributing significantly to turbulence suppression and confinement improvement.

Experimental investigations across stellarator devices have also confirmed the existence and importance of LFZF. In CHS, the first clear stellarator evidence of ZF was reported, with amplitudes enhanced in the presence of internal transport barriers [12]. In H-1, LFZF were shown to modulate radial electric field profiles and became stronger prior to the L-H transitions, consistent with energy transfer from turbulence [13]. TJ-II experimental studies have revealed long-range correlations (LRC) consistent with LFZF, showing amplitude scaling with stored energy and sensitivity to plasma heating schemes, as well as their capacity to modulate radial electric field shear [14-15]. In HSX, biasing experiments demonstrated the enhanced coherence and near-zero phase shift of low-frequency fluctuations, confirming the presence of ZF in quasi-helically symmetric configurations [16]. In TJ-K, ZF were observed to reduce turbulent particle transport by nearly 30%, primarily through phase decorrelation between density and potential fluctuations [17]. In LHD, long-range low-frequency fluctuations (~1-3 kHz) were found to propagate outward with velocities comparable to drift speeds, contributing significantly to transient transport [18]. More recently, W7-X provided the first direct observation of ZF in a large optimized stellarator, where they were shown to modulate local turbulence amplitudes, which is in agreement with gyrokinetic simulations [19]. Recent simulation studies have provided deeper insight into ZF dynamics in stellarators with various magnetic geometry. Nonlinear gyrokinetic studies indicated that ZF play a dominant role in turbulence saturation. *Tiwari et al.* demonstrated that ZF in W7-X and quasi-symmetric turbulence konzept (QSTK) provide strong suppression of ion heat flux, with QSTK exhibiting superior performance under steep gradients [20]. *Chen et al.* compared QA, QH, and QI geometries and showed that QH and QI benefit from higher residual levels and more effective nonlinear dynamics, resulting in stronger turbulence suppression, while QA configurations tend to exhibit weaker ZF regulation [21]. Residual zonal flows in helical systems are enhanced by the presence of equilibrium radial electric fields. This effect reduces damping and increases the long-time residual level of ZF [22]. Taken together, these nonlinear simulations emphasize that magnetic geometry has a decisive impact on ZF dynamics, that flux-tube approximations must be applied with caution in stellarators. *Sánchez et al.* highlighted that flux-tube simulations can misrepresent ZF relaxation in stellarators unless very long domains are used, while global simulations capture three-dimensional effects more reliably [23]. Similarly, *Smoniewski et al.* found that local models often distort ZF damping rates, reinforcing the need for global approaches [24].

These experimental and simulation works emphasize the central role of ZF in stellarator turbulent transport physics. Stellarator display a distinct transport behavior due to their three-dimensional magnetic geometry: neoclassical transport can be large and configuration-dependent, while turbulent transport is shaped by geometry, trapped-particle fraction, and drive mechanisms [25]. To reduce neoclassical losses, optimization strategies such as quasi-symmetry and ripple minimization have been proposed and developed [26-27]. The CFQS (Chinese First Quasi-axisymmetric Stellarator), designed to suppress neoclassical transport, thus provides a good platform to study turbulence-related physics, particularly the role of zonal flows, in a quasi-axisymmetric geometry [28-29]. Motivated by these pioneer works, the present study provides the first experimental evidence for zonal flow present in the optimized CFQS. *Nataka M. et al.* simulation work clearly demonstrates that the quasi-axisymmetric optimization of CFQS allows for robust ZF generation and regulation of turbulence [30]. However, despite these predictions, no experimental evidence of zonal flows in the optimized quasi-axisymmetric stellarator has yet been reported. The present study aims to provide the first experimental investigation into the existence and characteristics of zonal flows in CFQS, thereby testing theoretical predictions and offering new insights into turbulence regulation in advanced stellarator.

2. EXPERIMENTAL SETTINGS

The experiments were conducted on the Chinese First Quasi-axisymmetric Stellarator Test-device (CFQS-T) to investigate edge turbulence and flow dynamics. The CFQS-T is a low-aspect-ratio device (R = 1.0 m, a = 0.25 m) operated with a toroidal magnetic field of 0.05–0.1 T. Typical hydrogen (H) plasmas reached electron temperatures (T_e) of ~30-40 eV, while helium (He) plasmas exhibited slightly lower values, nearly ~20 eV. In the CFQS-T device, plasma heating is provided by a 2.45 GHz magnetron system. The system can deliver up to 15 kW of microwave power, offering sufficient flexibility for low-field operation and basic

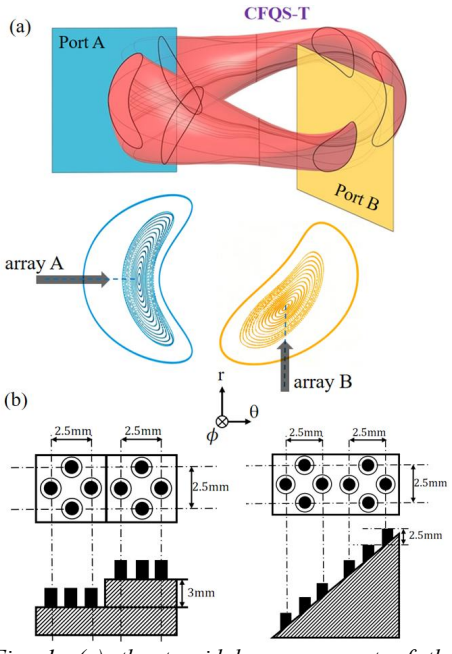

Fig. 1. (a) the toroidal arrangement of the probe arrays (array A and array B) and the corresponding magnetic surface configurations. (b) The sketch of double-step Langmuir probe and inclined double-step Langmuir probe.

turbulence studies. The line-averaged electron density ($n_{e,l}$) was ~ (4–5) × 10^{17} m^{-3}. Plasma parameters like floating potential (V_f), edge electron temperature (T_e) and electron density (n_e) and their fluctuations were measured using two Langmuir probe arrays, as illustrated in Figure 1 (a). One is the reciprocating probe system (array A), installed at the outer mid-plane (toroidal angle $\phi = 0°$), which can measure radial profiles of equilibrium and fluctuating parameters with a reciprocating velocity of ~0.1 m/s. Another is the stationary probe system (array B), mounted vertically upward from the bottom port (toroidal angle $\phi = 135°$), which can provide flexible radial fixed measurements and could be adjusted from shot to shot depending on the experimental requirements. Both probe arrays consisted of multiple tungsten tips with exposed length of 2.5 mm. Probe signals were sampled synchronously at 500 kHz with 16-bit digitizers, providing sufficient bandwidth to capture turbulence up to 250 kHz while retaining low-frequency flow dynamics. Two probe tips aligned along the magnetic field line were biased to 100 V to ensure reliable ion saturation current (Is) measurements based on the triple-tip principle [31]. Their spatial positioning was carefully adjusted according to the reconstructed magnetic geometry obtained from VEMC equilibrium calculations, ensuring consistency with the flux surface topology. This diagnostic configuration enabled systematic investigations of turbulence statistics, radial particle fluxes, and zonal flow characteristics in the edge plasma of CFQS-T.

3. EXPERIMENTAL RESULTS

3.1.Typical parameters evolution for one helium discharge

Figure 2 shows the temporal evolution of key diagnostic signals during a typical helium plasma discharge in CFQS-T, providing the background conditions for the study of low-frequency zonal flow (LFZF) dynamics. The magnetron power, displayed in Figure 2(a), is maintained at a stable level throughout the discharge but exhibits a distinct step increase at ~6000 ms. The line-integrated electron density ($n_{e,l}$), measured by microwave interferometry and shown in Figure 2(b), remains relatively stable during most of the discharge, with only a modest decrease following the magnetron step. Such a decrease in density is unclear, may be correlate with the change of power deposition profile during heating or the density pump-out effect [32]. Such stability ensures that the observed structures can be attributed to intrinsic plasma dynamics under nearly stationary background conditions. The Ha emission in Figure 2(c), monitoring neutral particle recycling, shows only minor variations, further confirming the absence of significant fueling effects before the ECH step. The radial position (Δ_{r1}) of probe array A is plotted in Figure 2(d), which expressed as the radial position from the last closed flux surface (LCFS). This movable probe array A inserts into the plasmas from +4cm to -14cm, while array B fixed at $\Delta_{r2} = -2cm$. Both arrays were operated with a sampling rate of 500 kHz, ensuring sufficient temporal resolution to capture the dynamics of LFZF structures, whose characteristic frequency lies in the kilohertz range. The high sampling frequency also guarantees accurate reconstruction of spectral features up to several hundred kHz, thereby excluding potential aliasing effects in the low-frequency domain. The spectral characteristics of the fluctuations are demonstrated in Figures 2(e) to (g). The power spectrum of $\tilde{V}_{f1}$ measured by array A in Figure 2(e) reveals a pronounced low-frequency oscillation at f ~ 1.0 kHz during 5500-6000 ms, consistent with the expected frequency band of LFZF and clearly distinct from geodesic acoustic modes (GAMs), which typically appear at higher frequencies in this magnetic field regime [2]. The cross-correlation spectrum shown in Figure 2(f) is calculated via two floating potentials ($\tilde{V}_{f1}$ and $\tilde{V}_{f2}$) toroidally separated 200 cm with a time window of 5ms, demonstrating there exists a zero-phase shift during the array A move inwards, indicating that the observed oscillation is a meso-scale structure extending along the toroidal direction with a finite radial localization. Finally, the magnetic

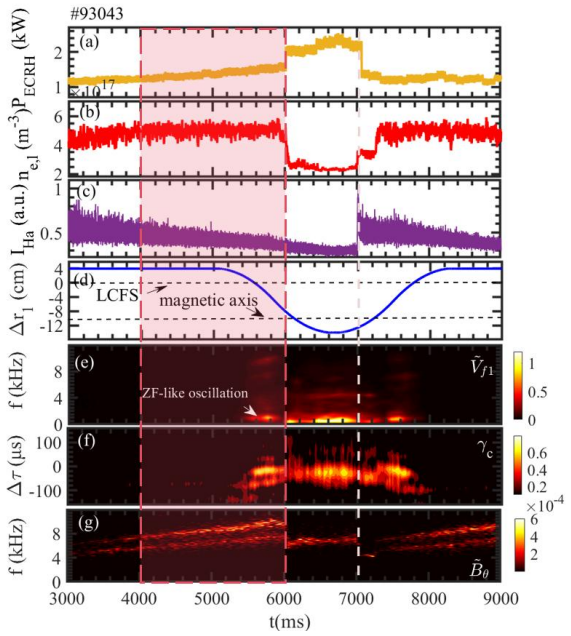

Figure 2. Temporal evolution of plasma parameters during a typical helium discharge in CFQS-T for shot #93043.(a) magnetron power, (b) line-integrated density ($n_{e,l}$), (c) Hα emission, (d) scanning trajectory of probe array A, (e) power spectrum of $\tilde{V}_{f1}$ measured by Array A, (f) γ_c between two toroidally separated floating potentials ($\tilde{V}_{f1}$ and $\tilde{V}_{f2}$) and (g) magnetic fluctuations ($\tilde{B}_\theta$). Focus phase for following analysis is highlighted by red shadow area.

fluctuation ($\widetilde{B}_\theta$) spectrum in Figure 2(g) exhibits no corresponding component < 4 kHz, ruling out an MHD origin and confirming the electrostatic nature of the mode. Besides, it should be noted that a supersonic molecular beam injection (SMBI) was applied at ~7000 ms to modify edge fueling. However, the present analysis focuses on the interval prior to 6000 ms, ensuring that the identified LFZF activity reflects intrinsic plasma behavior under relatively stationary discharge conditions. In summary, the coordinated analysis of global discharge parameters and high-resolution probe signals provides compelling evidence for the existence of LFZF-like structures in helium plasmas of CFQS-T.

3.2.Toroidal long-range correlation and radial structure of the LFZF

Following the identification of a distinct low-frequency oscillation in the floating potential spectrum shown in Figure 2, Figure 3 provides further evidence for its long-range toroidal correlation (LRC) between two floating potential signals separated by a toroidal distance of 200 cm for $\Delta t = 50ms$. The results are demonstrated in Figures 3(a)-(c), which present the cross-power spectrum, the cross-correlation spectrum, and the corresponding phase spectrum, respectively. The cross-power spectrum in Figure 3(a) reveals a pronounced spectral peak near 1.0 kHz, consistent with the frequency range of the LFZF identified previously. Figure 3(b) further confirms this feature by showing a strong and narrow correlation band at the same frequency, demonstrating that the oscillation remains coherent across the large toroidal separation. Complementing these results, Figure 3(c) shows that the relative phase between the two signals is nearly zero in this frequency band, indicating that the low-frequency oscillation structure extends long range along the toroidal direction without significant phase distortion. Taken together, these results establish that the observed 1.0 kHz oscillation is not a localized fluctuation but a long-range correlation characteristics mode, fully consistent with the defining properties of zonal flows [12-16]. The poloidal structure of the LFZF is examined in Figure 3(d) through the poloidal wave-number spectrum, i.e., S (k_θ,f) spectrum, calculated using two floating potential signals separated by 2.5 mm in the poloidal direction. The nearly zero poloidal wave number (k_θ) further confirms that the observed low-frequency oscillation is consistent with the nearly axisymmetric nature of LFZF. Finally, Figure 3(e) demonstrates the radial localization and width of the LFZF. To improve statistical reliability and reduce shot-to-shot variability, data from five reproducible discharges were combined. During each discharge, probe array A performed a controlled radial scan, and the floating potential signals were analyzed to compute the power spectrum at each radial location. The spectral amplitude integrated over the frequency range 0.5–1.5 kHz was used to construct the radial profile of LFZF amplitude. The resulting profile clearly identifies a finite radial width for $\Delta_r = -7cm \sim -3cm$, centered near a specific location at Δ_r = -5.5 cm, revealing that the LFZF is radially localized rather than extending uniformly across the edge plasma region Meanwhile, it is agreement with simulation result, which suggests that the LFZF localized at inner region while GAM localized at edge region[33], and it has been approved by several devices. The analysis above provides a comprehensive view of the LFZF's spatial characteristics and highlights the combined utility of toroidal correlation, poloidal structure, and radial profiling in diagnosing low-frequency, electrostatic zonal flows in quasi-axisymmetric stellarator.

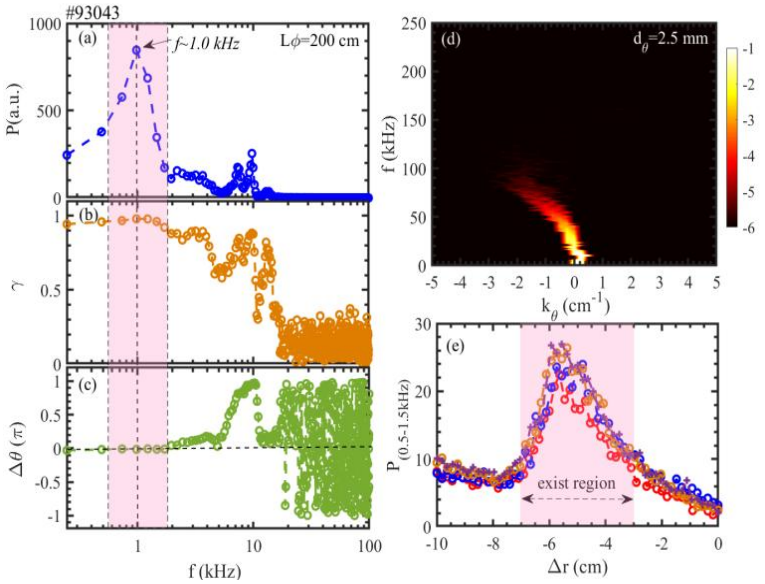

Fig. 3. Cross-power spectrum (a), coherence spectrum (b), and phase spectrum (c) of floating potential signals from two toroidally separated, (d) S (k_θ, f) spectrum of two poloidally separated $\widetilde{V}_f$, (e) Radial profile of LFZF amplitude from three reproducible discharges, with shaded bars indicating variability.

3.3. LFZF generation by nonlinear three-wave coupling

To further explore the underlying generation mechanism of the LFZF, nonlinear coupling analyses were

performed using bicoherence technique, which is defined as $b^2(f_1,f_2) = |B(f_1,f_2)|^2/[< |X(f_1)X(f_2)|^2 >< |X(f_3)X^*(f_3)|^2 >]$. In general, bicoherence analysis is widely used to investigate the generation mechanisms of coherent modes in plasmas, as it provides a quantitative measure of the phase coupling among different frequency components. Specifically, the squared bicoherence indicates the strength of three-wave interactions at frequency combinations, while the summed bicoherence offers a global, albeit approximate, measure of the overall nonlinear coupling in the system. In the present study, Figure 4(a) shows the squared bicoherence computed from the floating potential signals measured by the stationary probe on array B for $\Delta_t = 5000 - 6000\ ms$.

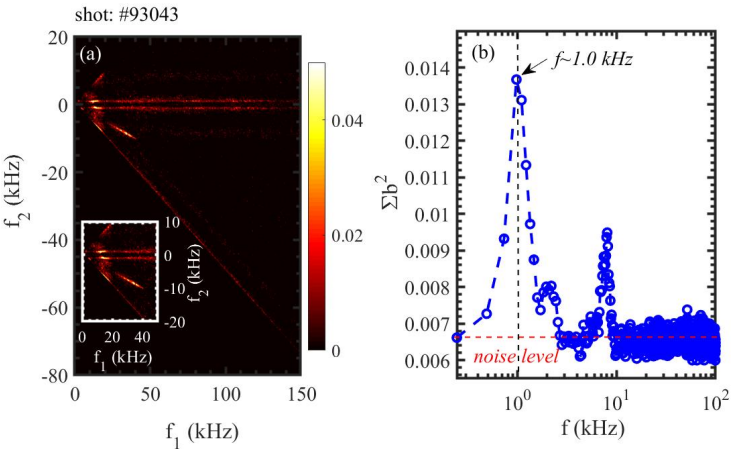

Fig. 4. (a) The contour of the squared auto-bicoherence of floating potential fluctuations <$\tilde{\phi}_f\tilde{\phi}_f\tilde{\phi}_f^*$> measured by Array B for Δ_t=5000-6000ms with a zomm-in image and (b) the resulting summed bicoherence $\sum b^2(f)$.

It is evident that the most significant nonlinearly coupling occurs within the low-frequency range of 10–150 kHz, indicating that the nonlinear interactions responsible for the coherent mode are predominantly associated with low-frequency turbulence. Furthermore, Figure 4(b) presents the summed bicoherence $\sum b^2(f)$ as a function of frequency, revealing a pronounced peak at f ≈ 1.0 kHz. This frequency coincides with the characteristic frequency of the LFZF identified in the previous analysis, suggesting that the LFZF is strongly linked to nonlinear energy transfer from the ambient turbulence, emerging from self-organization through three-wave coupling processes among turbulent fluctuations. These observations are consistent with theoretical predictions and previous experimental studies in other toroidal devices [6], where low-frequency zonal flows are generated via modulational instability and nonlinear interactions of background turbulence. By correlating the bicoherence analysis with the spectral characteristics of the floating potential, the present results provide compelling evidence that the LFZF in CFQS-T helium plasmas is sustained and regulated by the nonlinear coupling of ambient turbulence, highlighting the critical role of turbulence–zonal flow interactions in edge plasma dynamics.

3.4.Dynamical interactions between the LFZF and turbulent particle flux

Building on the evidence from the bicoherence analysis that the LFZF arises from nonlinear coupling of ambient turbulence, the next process is to investigate how the LFZF, once established, interacts with and regulates turbulent particle transport. Figure 5 provides a detailed view of this dynamic interaction in CFQS-T helium plasmas, highlighting the active role of the LFZF in modulating edge turbulence and corresponding radial transport (Γ_r). Figure 5(a) shows the turbulent particle flux (Γ_r) calculated using the four-probe array on array B with equation $\Gamma_r =< \tilde{n}_e \cdot \tilde{v}_r >$, providing a local measurement of cross-field transport in the plasma edge. The corresponding floating potential ($\tilde{V}_f^{env}$) is presented in Figure 5(b), representing the amplitude of the LFZF. Both signals were recorded at a sampling rate of 500 kHz to ensure sufficient temporal resolution for capturing the fast turbulence and the low-frequency zonal flow simultaneously. While the total analysis interval spans from 5000 to 6000 ms, the plots in (a) and (b) focus on a 20 ms zoomed-in window, allowing for a clearer visualization of the oscillatory dynamics and the relative phase relationship between the LFZF and flux transport. To quantify the modulation effect, the cross-correlation function (CCF) between the particle flux and the floating potential is shown in Figure 5(c). A pronounced central peak ($\gamma \sim -0.5$) in the CCF reveals a strong anti-phase relationship, indicating that

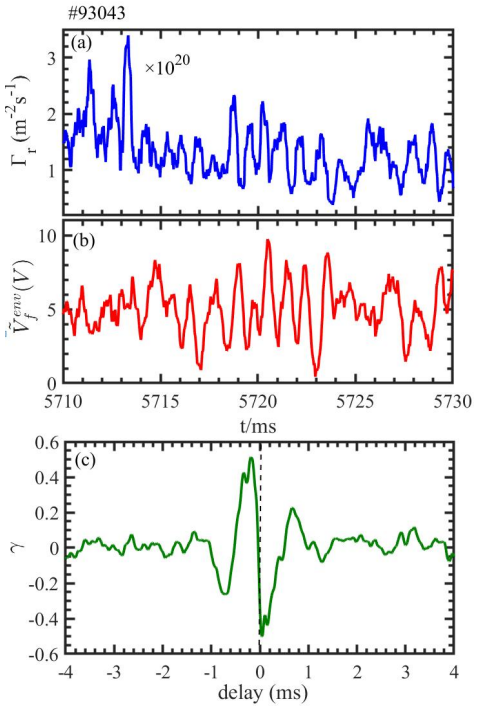

Fig. 5. (a) Turbulent particle flux (Γ_r) measured by the four-probe array on array B. (b) Floating potential ($\tilde{V}_f^{env}$) representing LFZF amplitude. (c) Cross-correlation function (CCF) between Γ_r and $\tilde{V}_f^{env}$.

peaks in the LFZF potential correspond to reductions in the local turbulent particle flux. This anti-correlation provides direct evidence that the LFZF actively suppresses turbulence-driven transport through shear-induced regulation of turbulent eddies. The modulation effect is consistent with previous experimental observations in tokamak [4,9] and stellarator [19] devices, where low-frequency zonal flows are known to mediate energy transfer from turbulent fluctuations, thereby reducing cross-field transport and contributing to the formation of transport barriers [12]. Moreover, the results in Figure 5 emphasize the spatial and temporal coherence of the LFZF in influencing turbulence. Overall, these observations demonstrate that LFZF in CFQS-T play a crucial role in regulating edge turbulence-driven particle transport, highlighting the fundamental importance of turbulence–zonal flow interactions in quasi-axisymmetric stellarators.

4. SUMMARY AND DISCUSSION

Low-frequency zonal flow (LFZF) in helium plasmas on CFQS-T were investigated by using two toroidally separated by 200 cm probe arrays. Floating potential measurements reveal a pronounced electrostatic oscillation at 1.0 kHz during a stationary discharge phase, exhibiting long-range toroidal coherence, finite wave number, and radial localization extend around -7cm to -3cm. Bicoherence analysis indicates that the this oscillation originates from nonlinear coupling with ambient turbulence, with the summed bicoherence peaking at the LFZF frequency, indicating a self-organized generation mechanism via three-wave interactions. Cross-correlation analysis further shows a clear inverse-phase relation between the LFZF potential and turbulent particle flux, demonstrating that LFZF regulate edge turbulence and mitigate cross-field transport, consistent with theoretical predictions of shear suppression and prior observations in other toroidal devices. This modulation confirms the essential role of LFZF in turbulence regulation and suggests their potential influence on transport barrier formation and overall confinement in CFQS-T. Building on these observations, further quantitative studies could focus on evaluating the turbulent Reynolds stress, estimating the energy transfer rate between turbulence and zonal flows, and calculating associated shearing rates. Future work should also investigate the dependence of LFZF amplitude and coherence on plasma parameters such as density, temperature, and magnetic field configuration, and explore isotope effects and scaling under higher heating power. These findings provide the first systematic experimental evidence of LFZF presence in CFQS-T helium plasmas, offering valuable benchmarks for turbulence and transport modeling in quasi-axisymmetric stellarator and advancing the understanding of turbulence–zonal flow interactions in low-field edge plasmas.

ACKNOWLEDGEMENTS

The This work is partially supported by the National Science Foundation of China under Grant No.12175186, and the Chinese National Fusion Project for ITER under Grant Nos. 2022YFE03070001, 2019YFE03040002 and 2019YFE03030002.

REFERENCES

[1] BURRILL, K. H., Turbulence and sheared flow, Science **281** (1998) 1816–1817.

[2] DIAMOND, P. H., ITOH, S. I., ITOH, K., et al., Zonal flows in plasma—a review, Plasma Phys. Control. Fusion **47** (2005) R35–R161.

[3] GUPTA, D. K., FONCK, R. J., MCKEE, G. R., et al., Detection of zero-mean-frequency zonal flows in the core of a high-temperature tokamak plasma, Phys. Rev. Lett. **97** (2006) 125002.

[4] LIU, A. D., LAN, T., YU, C.X., et al., Characterizations of low-frequency zonal flow in the edge plasma of the HL-2A tokamak, Phys. Rev. Lett. **103** (2009) 095002.

[5] HILLESHEIM, J. C., DELABIE, E., MEYER, H., et al., Stationary zonal flows during the formation of the edge transport barrier in the JET tokamak, Phys. Rev. Lett. **116** (2016) 065002.

[6] XU, G. S., WAN, B. N., SONG, M., et al., Direct measurement of poloidal long-wavelength E × B flows in the HT-7 tokamak, Phys. Rev. Lett. **91** (2003) 125001.

[7] NAGASHIMA, Y., HOSHINO, K., EJIRI, A., et al., Observation of nonlinear coupling between small-poloidal wave-number potential fluctuations and turbulent potential fluctuations in ohmically heated plasmas in the JFT-2M tokamak, Phys. Rev. Lett. **95** (2005) 095002.

[8] XU, Y., JACHMICH, S., WEYNANTS, R. R., et al., Long-distance correlation and zonal-flow structures induced by mean E × B shear flows in the biasing H-mode at TEXTOR, Phys. Plasmas **16** (2009) 110704.

[9] XU, G. S., WAN, B. N., WANG, H. Q., et al., First evidence of the role of zonal flows for the L-H transition at marginal input power in the EAST tokamak, Phys. Rev. Lett. **107** (2011) 125001.

[10] CZIEGLER, I., DIAMOND, P. H., FEDORCZAK, N., et al., Fluctuating zonal flows in the I-mode regime in Alcator C-Mod, Phys. Plasmas **20** (2013) 055904.

[11] SLADKOMEDOVA, A., CZIEGLER, I., FIELD, A. R., et al., Intermittency of density fluctuations and zonal-flow generation in MAST edge plasmas, J. Plasma Phys. 89 (2023) 905890614.

[12] FUJISAWA, A., ITOH, K., IGUCHI, H., et al., Identification of zonal flows in a toroidal plasma, Phys. Rev. Lett. **93** (2004) 165002.

[13] XIA, H., SHATS, M. G., PUNZMANN, H., et al., Strong ExB shear flows in the transport-barrier region in H-mode plasma, Phys. Rev. Lett. **97** (2006) 255003.

[14] KOBAYASHI, T., LOSADA, U., LIU B., et al., Frequency and plasma condition dependent spatial structure of low frequency global potential oscillations in the TJ-II stellarator, Nucl. Fusion **59** (2019) 044006.

[15] PEDROSA, M., SILVA, A.C., HIDALGO, C., et al., Evidence of Long-Distance Correlation of Fluctuations during Edge Transitions to Improved-Confinement Regimes in the TJ-II Stellarator, Phys. Rev. Lett. **100** (2008) 215003.

[16] WILCOX, R. S., VAN MILLIGEN, B.Ph., HIDALGO, C.,et al., Measurements of bicoherence and long-range correlations during biasing in the HSX stellarator, Nucl. Fusion **51** (2011) 083048.

[17] BIRKENMEIER, G.,RAMISCH, M., SCHMID, B., et al., Experimental Evidence of Turbulent Transport Regulation by Zonal Flows, Phys. Rev. Lett. **110** (2013) 145004.

[18] INAGAKI, S., TOKUZAWA, T., ITOH, K., et al., Observation of Long-Distance Radial Correlation in Toroidal Plasma Turbulence, Phys. Rev. Lett. **107** (2011) 115001.

[19] CARRALERO, D., ESTRADA, T., GARCÍA-REGANA, J. M., et al., First experimental observation of zonal flows in the optimized stellarator Wendelstein 7-X, Phys. Rev. Research **7** (2025) L022009.

[20] TIWARI, A., DAS, J., ALAGESHAN, J. K., et al., Zonal flow suppression of microturbulent transport in the optimized stellarators W7-X and QSTK, Plasma Phys. Control. Fusion **67** (2025) 085025.

[21] CHEN, H., WEI, X., ZHU, H., et al., Geometry effects on zonal flow dynamics and turbulent transport in optimized stellarators, Nucl. Fusion **65** (2025) 074002.

[22] SUGAMA, H., WATANABE, T.-H., Enhancement of residual zonal flows in helical systems with equilibrium radial electric fields, Contrib. Plasma Phys. **50** (2010) 571–575.

[23] SÁNCHEZ, E., GARCÍA-REGAÑA, J. M., BANÓN NAVARRO, A., et al., Gyrokinetic simulations in stellarators using different computational domains, Nucl. Fusion **61** (2021) 116074.

[24] SMONIEWSKI, J., SÁNCHEZ, E., CALVO, I., et al., Comparison of local and global gyrokinetic calculations of collisionless zonal flow damping in quasi-symmetric stellarators, Phys. Plasmas **28** (2021) 042503.

[25] XANTHOPOULOS, P., PLUNK, G.G., ZOCCO, A., et al., Intrinsic Turbulence Stabilization in a Stellarator, Phys. Rev. X **6** (2016) 021033.

[26] BEIDLER, C. D., SMITH, H. M., ALONSO, A., et al., Demonstration of reduced neoclassical energy transport in Wendelstein 7-X, Nature **596** (2021) 221–226.

[27] STROTH, U., FUCHERT, G., BEURSKENS, M.N.A., et al., Stellarator-tokamak energy confinement comparison based on ASDEX Upgrade and Wendelstein 7-X hydrogen plasmas, Nucl. Fusion **61** (2021) 016003

[28] LIU, H.F., SHIMIZU, A., XU, Y., et al., Configuration characteristics of the Chinese First Quasi-axisymmetric Stellarator, Nucl. Fusion **61** (2021) 016014.

[29] SHIMIZU, A., LIU, H.F., ISOBE, M., et al., Configuration property of the Chinese First Quasi-Axisymmetric Stellarator, Plasma Fusion Res. **13** (2018) 3403123.

[30] NAKATA, M., HONDA, M., NUNAMI, M., et al., The 27th International Toki Conference on Plasma and Fusion Research, 19–22 Nov. 2018 at Toki, Japan, **Oral presentation (ITC-27)**

[31] CHEN, S.L., SEKIGUCHI, T., Instantaneous Direct‐display system of plasma parameters by means of triple probe, J. Appl. Phys. **36** (1965) 2363‐2375.

[32] MAKINO, R., KUBO, S., IDO, T., et al.,Local and Fast Density Pump-out by ECRH in the LHD, Plasma Fusion Res. **8** (2013) 2402115

[33] MIYATO, N., KISHIMOTO, Y., LI, J., et al., Global structure of zonal flow and electromagnetic ion temperature gradient driven turbulence in tokamak plasmas, Phys. Plasmas **11** (2004) 5557 .